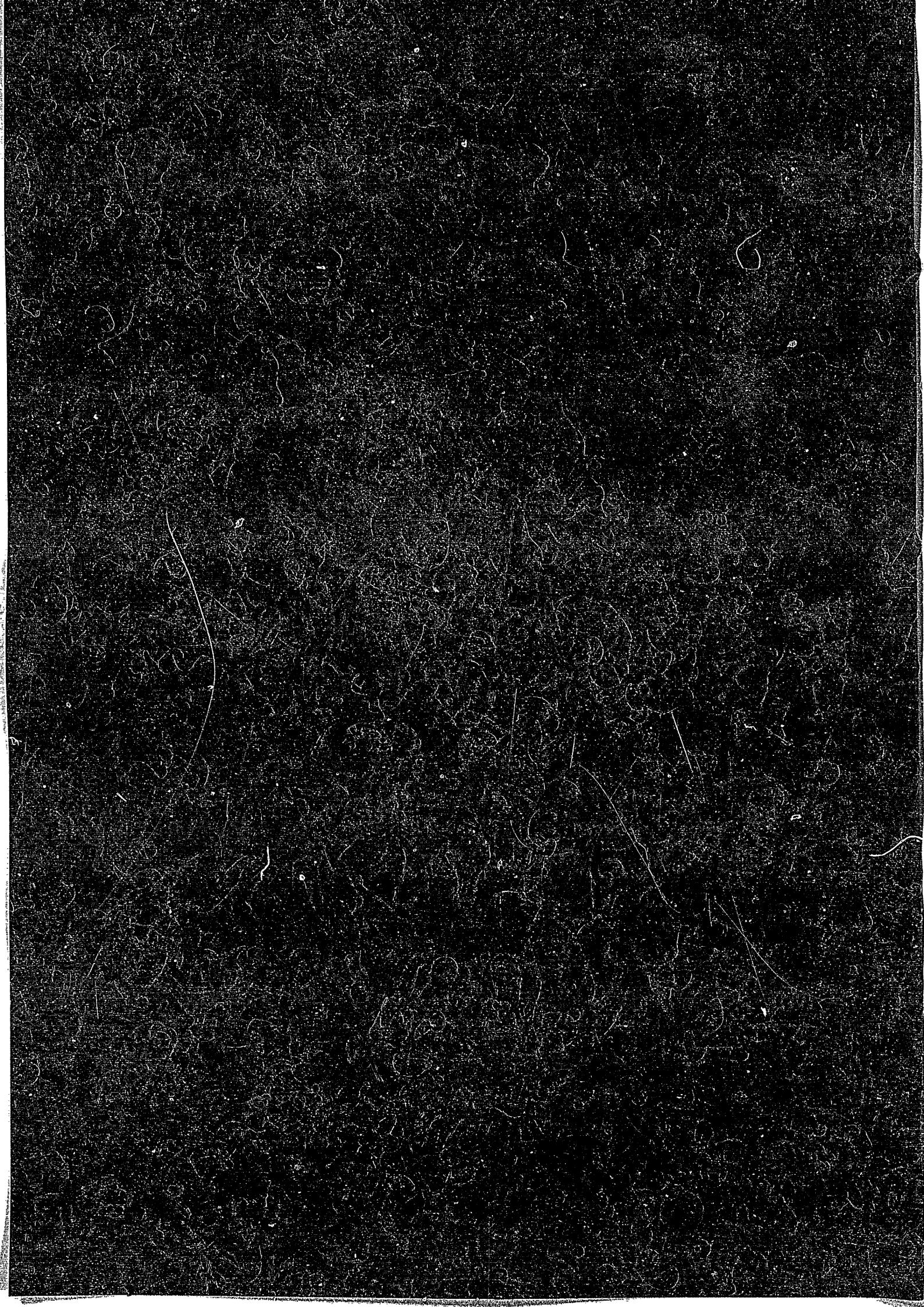


ENERGY DEPENDENCE OF ION-INDUCED SPUTTERING YIELDS
OF MONATOMIC SOLIDS IN THE LOW ENERGY REGION

N. MATSUNAMI, Y. YAMAMURA, H. ITOH
H. TAWARA AND T. KAWAMURA

INSTITUTE OF PLASMA PHYSICS
NAGOYA UNIVERSITY

NAGOYA, JAPAN



**ENERGY DEPENDENCE OF ION-INDUCED SPUTTERING YIELDS
OF MONATOMIC SOLIDS IN THE LOW ENERGY REGION**

N. Matsunami¹⁾, Y. Yamamura²⁾, N. Itoh³⁾, H. Tawara
and T. Kawamura

Institute of Plasma Physics, Nagoya University
Chikusa-ku, Nagoya 464, Japan

July 1987

Permanent address:

- 1) Department of Crystalline Materials Science, Faculty of Engineering,
Nagoya University, Nagoya 464, Japan
- 2) Department of Applied Physics, Faculty of Science,
Okayama University of Science, Okayama 700, Japan
- 3) Department of Physics, Faculty of Science, Nagoya University,
Nagoya 464, Japan

This document is prepared as a preprint of compilation of atomic data for fusion research sponsored fully or partly by the IPP/Nagoya University. This is intended for future publication in a journal or will be included in a data book after some evaluations or rearrangements of its contents. This document should not be referred without the agreement of the authors. Enquiries about copyright and reproduction should be addressed to Research Information Center, IPP/Nagoya University, Nagoya, Japan.

I. INTRODUCTION

Surfaces of solid materials are eroded under the energetic particle bombardment. This phenomenon is called sputtering. The erosion rate is characterized by the sputtering yield Y which is defined as the mean number of emitted atoms per incident particle. The sputtering yield depends in general on the type and state of the bombarded material, in particular the detailed structure and composition of the material surface, and the experimental geometry. There are a lot of review articles concerning with sputtering^{1,2,3,4}.

From the viewpoint of emission process, the sputtering can be classified into two categories; physical sputtering and chemical sputtering⁵. In physical sputtering, also called knockon sputtering, the sputtered particles receive enough energy from collisions with the incident particles to overcome the surface binding energy. The latter category invokes a chemical reaction induced by the impinging particles which produces an unstable compound at the surface. In this report the main concern is the physical sputtering. The physical sputtering is better understood than the chemical sputtering.

The physical sputtering is closely related to many of the topics in atomic collisions in solids¹. Subjects such as the interaction and penetration of ions in solids including range theory⁶, nuclear stopping and electronic stopping of particles in matter and the development of the radiation damage in materials have a bearing on sputtering. The Sigmund-Thompson^{7,8} theory based on the theory of nuclear stopping and radiation damage developed by Lindhard et al.⁶ provides the best theoretical framework to explain the basic aspects of the sputtering process. The transport theory of sputtering developed by Sigmund has shown to be powerful tool to understand the sputtering.

The physical model underlying the Sigmund-Thompson theory is as follows: An ion impinging on a random homogeneous solid generates a collision cascade, and recoiling atoms in the cascade will be sputtered when they reach the surface with sufficient energy to overcome the surface potential barrier U_s . The most significant results of the theory are expressed by the Thompson energy spectrum⁸

$$J(E, E_0) \propto E_0(E_0 + U_s)^3 \quad (1)$$

and by the Sigmund sputtering yield at normal incidence⁷

$$Y_S(E) = 0.042 \frac{\alpha (M_2/M_1) S_n(E)}{U_s} \quad (2)$$

where E is the ion energy, E_0 is the energy of a sputtered atom, $S_n(E)$ is the nuclear stopping cross section, and $\alpha (M_2/M_1)$ is a function of the mass ratio between the target mass M_2 and the ion mass M_1 .

Systematic deviations from the original Sigmund formula (2) have been pointed out for some cases, such as light-ion sputtering⁹ and low-energy sputtering¹⁰. After Sigmund's work, efforts have been made to get better expressions of sputtering yields from theories¹¹⁻¹³, empirical relations¹⁴⁻²⁰ and computer calculations²¹⁻³⁰.

Current needs for sputtering data at normal incidence and at oblique incidence have accelerated experimental measurements of sputtering yields. A useful and convenient presentation of these sputtering data is an empirical formula which is applicable to any ion-target combination and any incident energy. In views of plasma wall interaction, it is very important to estimate sputtering yields in the near threshold energy region.

In order to obtain a simple analytic expression for the purpose of the preliminary descriptions of unknown sputtering yields, Bohdansky et al. have proposed the following empirical formulae for sputtering yields in the near threshold energy regime at normal incidence^{15,16}:

$$Y_B = Q_B Y_N(E/E_{th}), \quad (3)$$

where $Y_N(y)$ is the reduced sputtering yield which has the form

$$Y_N(y) = 0.0085y^{1/4}[1 - y^{-1}]^{7/2} . \quad (4)$$

The fitting parameter Q_B and the threshold energy E_{th} employed in Eq. (4) are given by

$$Q_B = \begin{cases} 0.75M_2^{5/3} & M_1 < M_2 \\ 1 & M_1 > M_2 \end{cases} \quad (5)$$

$$E_{th} = \begin{cases} U_s/\gamma (1 - \gamma) & M_1/M_2 < 0.3 \\ 8U_s(M_1/M_2)^{2/5} & M_1/M_2 > 0.3 \end{cases} \quad (6)$$

where γ is the energy transfer factor which is defined as

$$\gamma = 4M_1M_2/(M_1 + M_2)^2. \quad (7)$$

Recently, Bohdansky revised the analytic formula of Eq. (3), and he obtained the following form¹⁸:

$$Y_B = Q_C s_n(\varepsilon) g(E/E_{th}). \quad (8)$$

Here $\varepsilon = E/E_L$ is the LSS reduced energy with the definition of

$$E_L = \frac{M_1 + M_2}{M_2} \frac{Z_1 Z_2 e^2}{a_L}, \quad (9)$$

where a_L is the Lindhard screening length⁶. In Eq.(8) Q_C is the so-called yield factor, which depends mainly on M_1 and M_2 and is independent of the incident energy, and $s_n(\varepsilon)$ is the reduced nuclear stopping cross section for which they used the following analytic approximation to the Thomas-Fermi model³¹ proposed by Matsunami et al.¹⁹:

$$s_n(\varepsilon) = \frac{3.441\sqrt{\varepsilon} \ln(\varepsilon + 2.718)}{1 + 6.355\sqrt{\varepsilon} + \varepsilon(6.882\sqrt{\varepsilon} - 1.708)}. \quad (10)$$

The function $g(y)$ is the correction factor for low ion energies

$$g(y) = (1 - y^{-2/3})(1 - y^{-1})^2. \quad (11)$$

The values of the yield factor Q_c are listed in refs. 4 and 18 for 68 ion-target combinations.

Under the joint research program of data compilation at the Research Information Center, Institute of Plasma Physics, the experimental data of the energy dependence of the sputtering yield at normal incidence were collected. Taking account of the threshold effect in the original Sigmund formula, the following empirical formula was proposed¹⁹:

$$Y = 0.042 \frac{\alpha S_n(E)}{U_s} [1 - (E_{th}/E)^{1/2}], \quad (12)$$

where E_{th} is the sputtering threshold energy and the sublimation energy is used as the surface binding energy U_s . The mass ratio dependences of α and the relative threshold energy $\xi = E_{th}/U_s$ are empirically determined in the form

$$\alpha = \begin{cases} 0.1019 + 0.0842(M_2/M_1)^{0.9805} & M_2/M_1 < 2.163 \\ -0.4137 + 0.6092(M_2/M_1)^{0.1708} & M_2/M_1 > 2.163, \end{cases} \quad (13)$$

and

$$\xi = \begin{cases} 4.143 + 11.46(M_2/M_1)^{-0.5005} & M_2/M_1 < 3.115 \\ 5.809 + 2.791(M_2/M_1)^{0.4816} & M_2/M_1 > 3.115. \end{cases} \quad (14)$$

The nuclear stopping cross section is given by

$$S_n(E) = Ks_n(\varepsilon), \quad (15)$$

where $s_n(\varepsilon)$ is given by Eq. (10) and K is the conversion factor from the reduced unit to the unit of $\text{eV cm}^2/10^{16}$ atoms:

$$K = 84.78 \frac{Z_1 Z_2}{(Z_1^{2/3} + Z_2^{2/3})^{1/2}} \frac{1}{M_1 + M_2}. \quad (16)$$

In 1984, a revised empirical formula was proposed by the same compilation group^{10,20}

$$Y = 0.042 \frac{\alpha^* Q(Z_2) S_n(E)}{U_s (1 + 0.35 U_s s_e(\varepsilon))} [1 - (E_{th}/E)^{1/2}]^{2.8}, \quad (17)$$

where $s_e(\varepsilon)$ is the Lindhard's inelastic stopping function³¹, and the empirical parameters α^* and E_{th} are given by

$$\alpha^* = 0.08 + 0.164(M_2/M_1)^{0.4} + 0.0145(M_2/M_1)^{1.29}, \quad (18)$$

and

$$\xi = E_{th}/U_s = 1.9 + 3.8(M_2/M_1)^{-1} + 0.134(M_2/M_1)^{1.24}. \quad (19)$$

The factor Q is the Z_2 -dependent parameter and is listed in Table 1.

The main concern of this report is the low-energy sputtering which is one of the most important processes for impurity release in fusion devices. The energies of ions and neutral atoms hitting the first wall are low and not in the energy range for which the original Sigmund formula is applicable. The empirical formulae mentioned above include the threshold effect, and for practical applications the threshold energy of sputtering yield must be known.

Using the Monte Carlo simulation code ACAT, Yamamura and Mizuno³⁰ investigated sputtering threshold energies at normal and oblique incidence, and derived the following mass ratio dependence of the rela

tive threshold energy at normal incidence:

$$\xi = E_{th}/U_s = 0.214 + 4.77(M_1/M_2)^{0.567} + 0.256(M_2/M_1). \quad (20)$$

For oblique incidence, however, it is very difficult to derive a universal relation for the threshold energy from computer studies³⁰.

In this report the theory of sputtering thresholds for not-too-oblique incidence will be developed, considering several collision sequences near the surface. A new version of the empirical formula is proposed in order to obtain the sputtering yield in the near threshold energy region.

II . THRESHOLD ENERGY FOR NOT-TOO-OBLIQUE INCIDENCE

Usually, the sputtering mechanism is classified into two parts³², i.e. the one due to collision cascades created by incoming ions (mechanism 1) and the other due to collision cascades generated by ions backscattered from the interior of solids (mechanism 2). The mechanism 1 is dominant for heavy-ion sputtering, while the mechanism 2 is dominant for light-ion sputtering.

Recent computer studies on low-energy sputtering indicate that for near threshold sputtering the sputtered atoms are generated by a few collisions and that all collision events take place only at the topmost layer and/or the second layer³⁰. The computer works of the sputtering²⁸ suggest the possible collision sequences which lead to near-threshold sputtering, which are shown in Figs. 1 and 2.

In the mechanism 1, the first primary recoil atom is sputtered or causes the sputtering process. In the mechanism 2, the projectile ion is scattered by target atoms inside solids, and create the primary recoil which is finally sputtered. Additional distinctions, A, B, C and D in Fig. 1 indicate that the number of collisions involved in the mechanism 1 are 1, 2, 3 and more than 4, respectively. Similarly, the number of collisions involved in the mechanism 2A, 2B and 2C in Fig. 2 are 1, 2 and more than 3, respectively.

First of all we calculate the 'threshold energy' for each collision sequence shown in Figs. 1 and 2 and identify the lowest energy as the real threshold energy³³.

2.1 Mechanism 1C

The mechanism 1C is the three-collision process for sputtering. This mechanism includes two different processes, i.e. ejection of the secondary recoil atom (mechanism 1C') and that of the primary recoil atom (mechanism 1C"). The former is important for small angles of incidence and the latter mechanism for large angles of incidence.

In Fig. 3, the more detailed descriptions of the mechanism 1C' and 1C" are shown, where E_0 is the energy of incidence and θ_0 is the angle of incidence measured from the surface normal. The energies, E_1 , E_2 , E_3 are those of the recoil atom after the first, second and third collisions, respectively. The total deflection angle measured from the surface normal after the first, second and third collisions are denoted by θ_1 , θ_2 and θ_3 , respectively.

For the mechanism 1C", each energy and total scattering angle is given as

$$E_1 = E_0 \gamma \sin^2(\Theta_1/2), \quad (21)$$

$$E_2 = E_1 [1 - \sin^2(\Theta_2/2)] = E_0 \gamma \sin^2(\Theta_1/2) \cos^2(\Theta_2/2), \quad (22)$$

$$\begin{aligned} E_3 &= E_2 [1 - \sin^2(\Theta_3/2)] \\ &= E_0 \gamma \sin^2(\Theta_1/2) \cos^2(\Theta_2/2) \cos^2(\Theta_3/2), \end{aligned} \quad (23)$$

$$\theta_1 = \theta_0 + (\pi - \Theta_1)/2, \quad (24)$$

$$\theta_2 = \theta_1 + \Theta_2/2 = \theta_0 + (\pi - \Theta_1 + \Theta_2)/2, \quad (25)$$

$$\theta_3 = \theta_2 + \Theta_3/2 = \theta_0 + (\pi - \Theta_1 + \Theta_2 + \Theta_3)/2, \quad (26)$$

where Θ_1 , Θ_2 and Θ_3 are the scattering angles in the center of mass (CM) system.

Replacing Θ_2 by $\pi - \Theta_2$ in Eqs. (22) and (25), we can easily get the energies and the total scattering angles of the secondary recoil atom of the mechanism 1C'. This means that the formula for threshold energy of the mechanism 1C' is the same as that of the mechanism 1C", because the second and third collisions are equal-mass collisions.

Here, we obtain the vertical component E_+^{1C} of the energy of the outgoing recoil atom, which has the form

$$E_+^{1C} = E_0 \gamma \sin^2(\Theta_1/2) \cos^2(\Theta_2/2) \cos^2(\Theta_3/2) \times \sin^2\left(\theta_0 - \frac{\Theta_1 - \Theta_2 - \Theta_3}{2}\right). \quad (27)$$

Here, we use the planar potential as the surface barrier for the sputtering. Then, the 'threshold energy' of the mechanism 1C is given by setting the maximum value of E_+^{1C} be equal to the surface binding energy. Rigorously speaking, the CM scattering angles in Eq. (27) are functions of the impact parameter p_1 of Fig. 3, if the configuration of each target atom is fixed. However, the purpose of this report is to obtain the threshold energy in a random target. Therefore, it is very reasonable to assume that any configuration of target atoms is allowed for the threshold sputtering. This assumption tells us that the three CM scattering angles, Θ_1 , Θ_2 and Θ_3 , are independent variables.

If we accept the above-mentioned assumption, it is very easy to obtain the maximum value of E_+^{1C} . We have only to differentiate E_+^{1C} with respect to Θ_1 , Θ_2 and Θ_3 , and using the conditions of $\delta E_+^{1C}/\delta \Theta_3 = 0$, $\delta E_+^{1C}/\delta \Theta_2 = 0$ and $\delta E_+^{1C}/\delta \Theta_1 = 0$, we have the following simple relations for the maximum value of E_+^{1C} :

$$\Theta_3 = (\pi - 2\theta_0 + \Theta_1 - \Theta_2)/2, \quad (28)$$

$$\Theta_2 = (\pi + \Theta_1 - 2\theta_0)/3, \quad (29)$$

$$\Theta_1 = (\pi + \theta_0)/2. \quad (30)$$

Substituting Eqs. (28), (29) and (30) into Eq. (27) yields the maximum vertical component of the energy of the outgoing recoil atom

$$E_+^{1C} = E_0 \gamma \sin^8 \frac{\pi + \theta_0}{4}. \quad (31)$$

The 'threshold energy' is equal to the energy of incidence when the equality $E_{+1C} = U_s$ is held. Then, we obtain the 'threshold energy' of the mechanism 1C, i.e.

$$E_{th}^{1C} = \frac{U_s}{\gamma \sin^8 \frac{\pi + \theta_0}{4}} \quad (32)$$

It is of interest to know the physical conditions which give the threshold collision sequence. First of all let us consider the scattering angle in the laboratory (L) system at each collision. With help of the relations obtained in Eqs. (28), (29) and (30), some algebraic arrangements give a simple relation

$$\theta_1^L = \theta_2^L = \theta_3^L = \frac{\pi - \theta_0}{4} \quad (33)$$

These equalities means that the threshold collision sequence or the minimum energy-loss process, is the collision sequence of the equal-angle scatterings.

The sputtered atom loses the vertical component of its energy by an amount of U_s to overcome the surface barrier. At the threshold energy, hence, the sputtered atom is emitted parallel to the surface. This is effectively a deflection due to the surface barrier. Its deflection angle θ_{def} is equal to $(\pi - \theta_0)/4$, and the supplement of θ_{def} is equal to the scattering angle of the minimum energy-loss sequence. Then, we have

$$\theta_1^L + \theta_2^L + \theta_3^L + (\pi/2 - \theta_{def}) = \pi - \theta_0 \quad (34)$$

The schematic representation of the minimum energy-loss sequence is shown in Fig. 4.

2.2 Mechanism 1D.

The mechanism 1D is the generalized case of the mechanism 1 (see Fig. 5). After the first collision the primary recoil atom is produced and it experiences m collisions before it knocks off a surface atom. As

was already mentioned in the previous section, the production of the higher-order recoil atom is equivalent to the scattering of the primary recoil atom due to the equal mass collision from the viewpoint of threshold energy.

The conclusion of the previous section is that the collision sequence with the equal-scattering-angle gives the maximum value for the vertical component of the outgoing particle. The same conclusion holds for the successive $(m + 2)$ collision process in the mechanism 1D, while the deflection angle due to the surface barrier has the following expression:

$$\theta_{\text{def}} = \theta_0 - \Theta_1/2 + (m + 2)\Theta_m/2. \quad (35)$$

Using the requirement that all scattering angles at each collision and the supplementary angle of θ_{def} are equal and using the relation of Eq. (34), we can determine the CM scattering angle at the first collision and we have the following equations similar to Eq. (33):

$$\theta_m^L = \frac{\pi - \Theta_1}{2} = \frac{\Theta_m}{2} = \frac{\pi}{2} - \theta_{\text{def}} = \frac{\pi - \theta_0}{m + 4}. \quad (36)$$

Here, θ_m^L is the scattering angle in the L system.

This minimum energy-loss condition gives an explicit expression for the 'threshold energy' of the mechanism 1D

$$E_{\text{th}}^{1D} = \frac{U_s}{\gamma \sin^{2m+8} \frac{(m+2)\pi + 2\theta_0}{2m + 8}}. \quad (37)$$

The minimum energy-loss condition of this mechanism is schematically shown in Fig. 6. Note that for $m = 0$ this equation is reduced to Eq. (32).

2.3 Mechanism 2C

The mechanism 2A and mechanism 2B are the special cases of the mechanism 2C. Let us discuss the threshold energy of the mechanism 2C. The schematic representation of the mechanism 2C is shown in Fig. 7. The moving particle in a solid is the projectile. After the first collision, the projectile makes m equal-angle scatterings with target atoms before it kicks off a surface atom which is finally sputtered.

After the first collision, the energy E_1 and the total scattering angle θ_1 are given as

$$E_1 = E_0 \{1 - \gamma \sin^2(\theta_1/2)\}, \quad (38)$$

$$\theta_1 = \theta_0 + \theta_{12}^L, \quad (39)$$

where

$$\theta_{12}^L = \tan^{-1} \frac{\sin \theta_1}{\mu + \cos \theta_1} \quad (40)$$

with the definition of $\mu = M_1/M_2$.

The energy E_{m+1} and the total scattering angle θ_{m+1} before producing the primary recoil atom are

$$E_{m+1} = E_0 \{1 - \gamma \sin^2(\theta_1/2)\} \{1 - \gamma \sin^2(\theta_m/2)\}^m, \quad (41)$$

$$\theta_{m+1} = \theta_0 + \theta_{12}^L + m\theta_m^L, \quad (42)$$

where θ_m^L is the scattering angle in the L system for the equal-angle scattering and θ_m is the corresponding scattering angle in the CM system.

The energies E_{m+2} and E_{m+3} and the total scattering angles θ_{m+2} and θ_{m+3} of the primary recoil atom are given as

$$E_{m+2} = E_{m+1} \gamma \sin^2(\theta_{m+2}/2), \quad (43)$$

$$E_{m+3} = E_{m+2} \{1 - \sin^2(\Theta_{m+3}/2)\} , \quad (44)$$

$$\theta_{m+2} = \theta_{m+1} + (\pi - \Theta_{m+2})/2, \quad (45)$$

$$\theta_{m+3} = \theta_{m+2} + \Theta_{m+3}/2 . \quad (46)$$

The vertical component of the energy of the outgoing recoil atom has the expression

$$E_+^{2C} = E_0 \gamma \{1 - \gamma \sin^2(\Theta_1/2)\} \{1 - \gamma \sin^2(\Theta_m/2)\}^m \\ \times \sin^2(\Theta_{m+2}/2) \cos^2(\Theta_{m+3}/2) \\ \times \sin^2 \{ \theta_0 + \theta_{12}^L + m\theta_m^L - (\Theta_{m+2} - \Theta_{m+3})/2 \} . \quad (47)$$

Here we assume again that the atomic configuration is random as in Section 2.1. By differentiating E_+^{2C} with respect to the independent variables $\Theta_1, \Theta_m, \Theta_{m+2}$ and Θ_{m+3} , we get the 'threshold energy' of the mechanism 2C:

$$E_{th}^{2C} = \frac{U_g (1 + \mu)^{2m+2} (1 + 2\mu \cos \Theta_1 + \mu^2)^{2-m}}{\gamma (1 + \mu \cos \Theta_1)^6} , \quad (48)$$

where Θ_1 is the solution of the following transcendental equation:

$$(m + 1)\theta_{12}^L + 3\theta_{21}^L = \pi - \theta_0 . \quad (49)$$

and the scattering angle θ_{21}^L is defined as

$$\theta_{21}^L = \tan^{-1} \frac{\mu \sin \Theta_1}{1 + \mu \cos \Theta_1} \quad (50)$$

The factor $(m + 1)$ in Eq. (49) means the number of equal-angle scattering angles, while the factor 3 of θ_{21}^L means the sum of two equal-angle collisions of the primary recoil atom and the supplementary angle of the deflection angle θ_{def} due to the surface barrier.

The angle θ_{21}^L is the recoil angle when the primary recoil atom is produced, and it is equal to the L scattering angle between a moving recoil atom and a projectile at rest. Then, we have

$$\theta_{12}^L + \theta_{21}^L = \Theta_1 \quad (51)$$

The minimum energy-loss process of the mechanism 2C is interpreted as the following: 1) A projectile follows the equal-scattering-angle collision sequence, 2) a produced primary recoil atom also makes the equal-scattering-angle collision sequence, 3) the sum of the L scattering angle of the projectile and its recoil angle is equal to the CM scattering angle at the collision which produces the primary recoil atom, and 4) the supplementary angle of the deflection angle is equal to the L scattering angle of the collision sequence of the primary recoil atom.

Since the transcendental equation (49) cannot be solved analytically except for $m = 2$, the following approximate formula is very useful in the whole region of μ

$$E_{\text{th}}^{2C} = \frac{U_s}{\gamma} \frac{1}{\cos^6 \theta_a} \left[\frac{1 + \mu}{\cos \theta_a + \mu \cos(\theta_a/\mu)} \right]^{2m+2} \quad (52)$$

where

$$\theta_a = \frac{\mu (\pi - \theta_0)}{m + 1 + 3\mu} \quad (53)$$

Finally, we determine the real threshold energy of sputtering. For $M_1 = M_2$, E_{th}^{1D} is equal to E_{th}^{2C} for the same collision number m . The 'threshold energy' of the mechanism 1D is symmetric with respect to $M_1 = M_2$, and simple arithmetic calculations yield

$$E_{th} = \begin{cases} E_{th}^{1D} & M_1 > M_2 \\ E_{th}^{2C} & M_1 < M_2 \end{cases} \quad (54)$$

This equation tells us that the real threshold process corresponds to the collision sequence where a particle with the smaller mass is moving inside the solid.

III . THE EMPIRICAL FORMULA WITH REVISED EMPIRICAL PARAMETERS

The threshold energies derived in Section II are applicable to oblique incidence. Due to the scarcity of data for the oblique incidence, data for the normal incidence is treated hereafter. In the previous reports^{19,20} empirical parameters α^* , Q and E_{th} of Eq. (17) are determined at the same time using a non-linear least square method for whole energy regions. No significant weight was placed for the low energy region, resulting in a little bit scatter of the E_{th} values. However, it is better to determine these empirical parameters independently.

In this report, better E_{th} values are obtained using the following method for the low energy region. We define the reduced sputtering yield Y^* by³⁴

$$Y^* = E^{1/2} \{Y/S_n^*(E)\}^{1/2.8}, \quad (55)$$

and we have from Eq. (17)

$$Y^* = A(\sqrt{E} - \sqrt{E_{th}}), \quad (56)$$

Here A is an energy-independent parameter which includes the empirical parameter α , and $S_n^*(E)$ is the effective nuclear stopping cross section

which is defined as

$$S_n^*(E) = \frac{S_n(E)}{1 + 0.35U_s s_e(\varepsilon)} \quad (57)$$

We have carried out the linear fitting of the sputtering data of 205 ion-target combinations to Eq. (55) for $S_n(E) < 2.5 \times 10^{-13}$ eV.cm². That is to say, in the Y^* versus \sqrt{E} plot, the threshold energy E_{th} is the intersection and the parameter α is proportional to the slope.

In Fig. 8, we compared threshold energies determined empirically with theory. Almost empirical threshold energies lie between the $m = 1$ curve and the $m = 2$ curve. In this report we adopted the $m = 2$ threshold energy, i.e.

$$E_{th} = \begin{cases} \left(\frac{4}{3} \right) \frac{6 U_s}{\gamma} & M_1 \cong M_2 \\ \frac{U_s}{\gamma} \left(\frac{2M_1 + 2M_2}{M_1 + 2M_2} \right)^6 & M_1 \cong M_2 \end{cases} \quad (58)$$

As in the previous paper¹⁰, α is expressed as α^*Q . Figure 9 shows empirical parameters α^* as a function of the mass ratio M_2/M_1 . The solid line in Fig. 9 is the revised empirical value of α^*

$$\alpha^* = 0.10 + 0.155(M_2/M_1)^{0.73} + 0.001(M_2/M_1)^{1.5} \quad (59)$$

The Q values of Eq. (17) depend primary on the target materials and are determined as the average of α/α^* over ions. The revised Q values are listed in Table 2.

IV. COMPARISON OF THE EMPIRICAL FORMULA WITH EXPERIMENTAL DATA

The energy dependence of the sputtering yield of all available combinations of incident ions and target atoms upto 1983 have been compiled and stored in the computer²⁰. The comparisons between measured sputtering yields and the present empirical formula (17) are given in Figs. 10 through 14, where α^* is calculated using the revised empirical relation (59), the threshold energy is calculated from the theoretical formula Eq.(58), and as Q values we used those of Table 2.

Agreement between the solid curve and data points for each ion-target combination have been improved especially for the low-energy region as compared with the previous empirical works²⁰ with Eqs. (18) and (19), except for H, D and He ions on Be target. More careful studies are required to investigate the poor agreement for Be target. It should be noted that the E_{th} values are smaller than those in the previous report²⁰ and hence the sputtering yields are non-zero for very low energies.

REFERENCES

- 1) P. Sigmund, Rev. Roum. Phys. 17 (1972) 1079.
- 2) P. Sigmund, "Inelastic Ion-Surface Collisions", eds. by N.H. Tolk, J.C. Tully, W. Heiland and C.W. White, Academic Press, New York, 1977, p121.
- 3) H.H. Andersen and H.L. Bay, "Sputtering by Particle Bombardment I, ed. R. Behrisch. Springer-Verlag, Berlin, 1981.
- 4) J. Bohdansky, "Data Compendium for Plasma-Surface Interactions", IAEA, Vienna, 1984, p61.
- 5) J. Roth, "Data Compendium for Plasma-Surface Interactions", IAEA, Vienna, 1984, p72.
- 6) J. Lindhard, V. Nielsen, M. Scharff and P.V. Thomsen, Dan. Vid. Selsk. Mat. Fys. Medd. 36 (1963) No. 10.
- 7) P. Sigmund, Phys. Rev. 184(1969) 383.
- 8) M.W. Thompson, Phil. Mag. 18 (1968) 377.
- 9) U. Littmark and S. Fedder, Nucl. Instr. Meth. 194 (1982) 607.
- 10) Y. Yamamura, N. Matsunami and N. Itoh, Rad. Eff. 71 (1983) 65.
- 11) G. Falcone, Phys. Rev. B33 (1986) 5054.
- 12) M.M.R. Williams, Progress in Nuclear Energy, 3 (1979) 1.
- 13) M.H. Urbassek, Nucl. Instr. Meth. B4 (1984) 356; Nucl. Instr. Meth. B6 (1985) 585.

- 14) D.L. Smith, Proc. Workshop on Sputtering Caused by Plasma Surface Interactions, Conf-790775, 15-1 (1980).
- 15) H.L. Bay, J. Roth and J. Bohdansky, J. Appl. Phys. 48 (1977) 4722.
- 16) J. Bohdansky, J. Roth and H.L. Bay, J. Appl. Phys. 51 (1980) 2861.
- 17) J. Bohdansky, J. Nucl. Mater. 93/94 (1980) 44.
- 18) J. Bohdansky, Nucl. Instr. Meth. B2 (1984) 587.
- 19) N. Matsunami, Y. Yamamura, Y. Itikawa, N. Itoh, Y. Kazumata, S. Miyagawa, K. Morita and R. Shimizu, IPPJ-AM-14, Institute of Plasma Physics, Nagoya University, 1980.
- 20) N. Matsunami, Y. Yamamura, Y. Itikawa, N. Itoh, Y. Kazumata, S. Miyagawa, K. Morita, R. Shimizu and H. Tawara, IPPJ-AM-32, Institute of Plasma Physics, Nagoya University, 1984, see also Atomic Data Nucl. Data Tables 31 (1984) 1.
- 21) Y. Yamamura and K. Kitazoe, Rad. Eff. 39 (1978) 251.
- 22) T.J. Hoffmann, H.L. Dodds, Jr., M.T. Robinson and D.K. Holmes, Nucl. Sci. Eng. 68 (1978) 204.
- 23) D.E. Harrison, N.S. Levy, J.P. Johnson, III and H.M. Effron, J. Appl. Phys. 39 (1968) 3742.
- 24) D.E. Harrison, Jr., J. Appl. Phys. 53 (1982) 4193; Nucl. Instr. Meth. 218 (1983) 727.
- 25) V.E. Yurasova and V.A. Eltekov, Proc. Symposium on Sputtering, Dercholdsdorf/Wien, Austria (1980) p134.
- 26) L.G. Haggmark and W.D. Wilson, J. Nucl. Mater. 76/77 (1978) 149.
- 27) J.P. Biersack and L.G. Haggmark, Nucl. Instr. Meth. 174(1980) 257.
- 28) J.P. Biersack and W. Eckstein, Appl. Phys. A34 (1984) 73.
- 29) M.T. Robinson and I.M. Torrens, Phys. Rev. B9 (1974) 5008.
- 30) Y. Yamamura and Y. Mizuno, IPPJ-AM-40, Institute of Plasma Physics, Nagoya University (1985).
- 31) J. Lindhard, M. Scharff and Schiøtt, Dan. Vid. Selsk. Mat. Fys. Medd. 33 (1963) No. 14.
- 32) R. Weissmann and R. Behrisch, Rad. Eff. 19 (1973) 69.
- 33) Y. Yamamura and J. Bohdansky, Vacuum 35 (1985) 561.
- 34) Y. Yamamura and Y. Mizuno, Nucl. Instr. Meth. 128/129 (1984) 559.
- 35) J. Roth, J. Bohdansky and W. Ottenberger, Report IPP-9/26, Max-Planck Institut für Plasmaphysik (1979).
- 36) H. Fetz and H. Oechsner, Proc. 6th Conf. Ionized phenomena in Gases, Paris Vol. II (1961) p39.
- 37) D. Rosenberg and G.K. Wehner, J. Appl. Phys. 33 (1962) 1842.
- 38) N. Laegreid and G.K. Wehner, Trans. 6th Nat. Vacuum Symposium, Pergamon (1959) p164.
- 39) A.K. Furr and C.R. Finfgeld, J. Appl. Phys. 41 (1970) 1739.

- 40) H.H. Andersen and H.L. Bay, J. Appl. Phys. 46 (1974) 2416.
- 41) J.S. Colligon and R.W. Bramham, Atomic Col. Solids, Brighton (1970) p258.
- 42) N. Laegreid and G.K. Wehner, J. Appl. Phys. 32 (1961) 365.
- 43) R. Behrisch, J. Bohdansky, G.H. Oetjen, J. Roth, G. Schilling and H. Verbeek, J. Nucl. Mater. 60 (1976) 321.
- 44) J. Roth, J. Bohdansky and K.L. Wilson, J. Nucl. Mater. 111/112 (1982) 775.
- 45) J.N. Smith, C.H. Meyer and J.K. Layton, Nucl. Technol. 29 (1976)318.
- 46) J.N. Smith, C.H. Meyer and J.K. Layton, J. Nucl. Mater. 67 (1977) 234.
- 47) M. Yamashita, S. Baba and A. Kinbara, J. Vac. Soc. Japan 25 (1982) 249.
- 48) G. Betz, R. Dobrozemaky, F.P. Veshbock and H. Wotke, Proc. 9th Int. Conf. Phenomena Ionized Gases, Bucharest, p91.

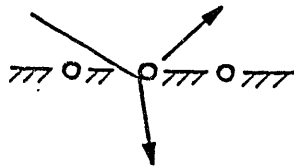
Table 1 Q values of the empirical formula (17)

target	Q	target	Q	target	Q
Be	2.17	Ni	1.06	Hf	0.75
B	4.6	Cu	1.30	Ta	0.78
C	3.1	Ge	0.83	W	1.10
Al	1.09	Zr	0.70	Re	1.27
Si	0.78	Nb	1.02	Os	1.47
Ti	0.58	Mo	0.84	Ir	1.37
V	0.90	Ru	1.52	Pt	1.13
Cr	1.23	Rh	1.26	Au	1.04
Mn	1.13	Pd	1.10	Th	0.90
Fe	1.06	Ag	1.21	U	0.81
Co	1.00	Sn	0.47		

Table 2 Revised empirical Q values for the empirical formula (17)

target	Q	target	Q	target	Q
Be	1.97	Ni	0.94	Hf	0.65
B	4.10	Cu	1.27	Ta	0.62
C	2.69	Ge	0.73	W	0.77
Al	1.11	Zr	0.68	Re	1.34
Si	0.95	Nb	1.02	Os	1.47
Ti	0.58	Mo	0.70	Ir	1.39
V	0.76	Ru	1.51	Pt	0.93
Cr	1.03	Rh	1.23	Au	1.02
Mn	1.09	Pd	1.09	Th	0.73
Fe	0.90	Ag	1.24	U	0.66
Co	0.98	Sn	0.58		

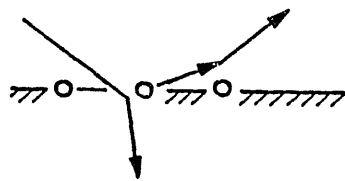
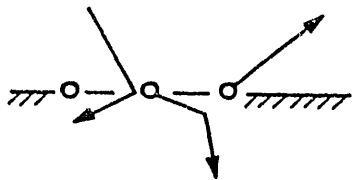
MECHANISM 1



MECHANISM 1A

1B'

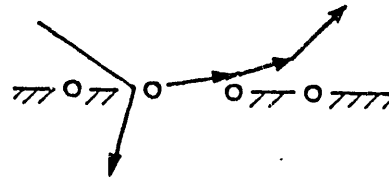
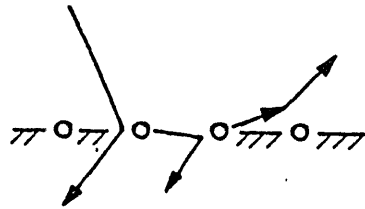
1B''



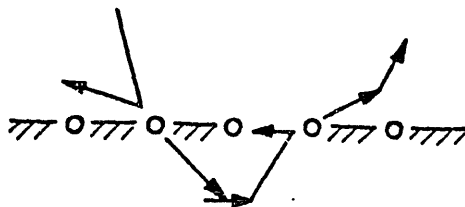
MECHANISM 1B

1C'

1C''



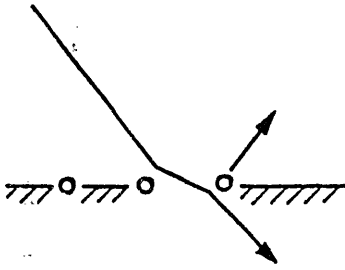
MECHANISM 1C



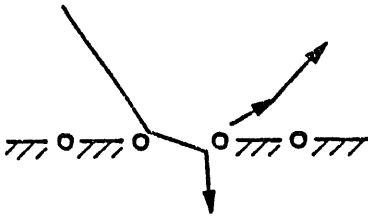
MECHANISM 1D

Fig. 1 Possible mechanisms for the threshold sputtering of heavy ions, where a primary recoil atom is produced at the first collisions.

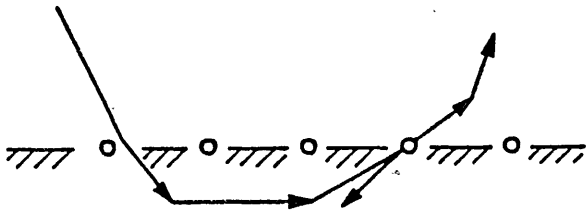
MECHANISM 2



MECHANISM 2A



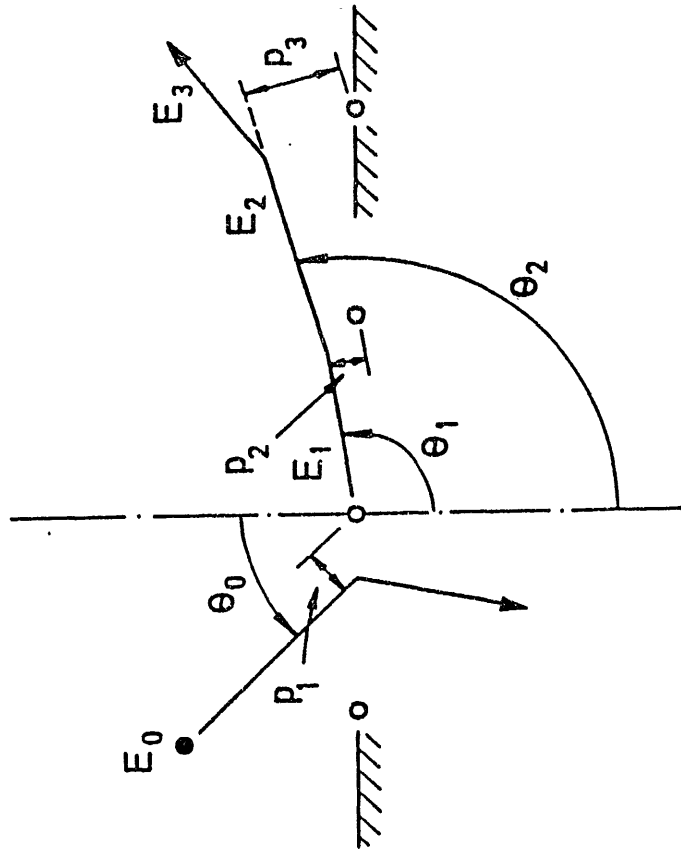
MECHANISM 2B



MECHANISM 2C

Fig. 2 Possible mechanisms for the threshold sputtering of light ions, where a primary recoil atom is produced after several collisions of the projectile.

MECHANISM 1C''



MECHANISM 1C'

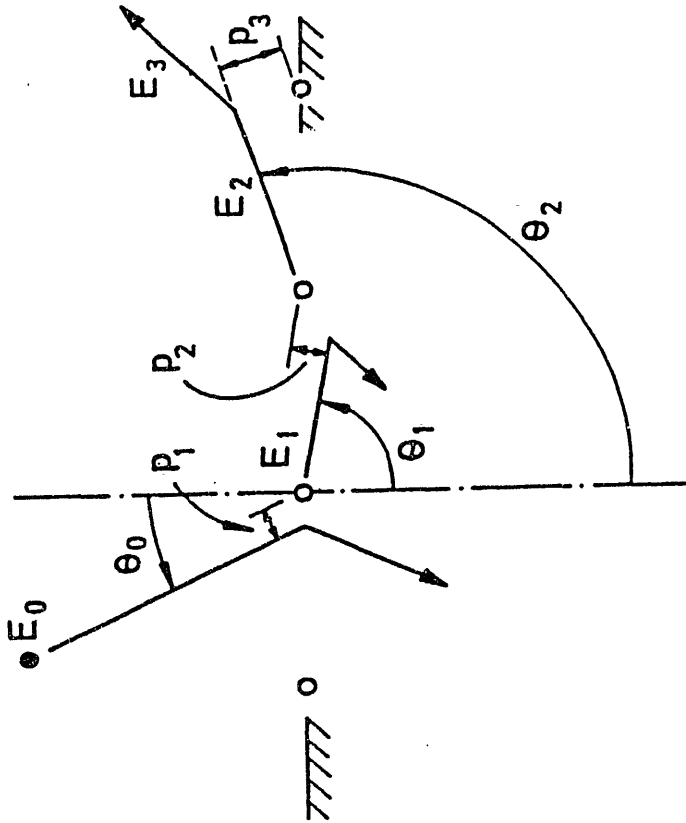


Fig. 3 Schematic representations of a three collisions process of the mechanism 1C' and the mechanism 1C''. In the mechanism 1C' the secondary recoil atom is sputtered, while in the mechanism 1C'' the primary recoil atom is sputtered.

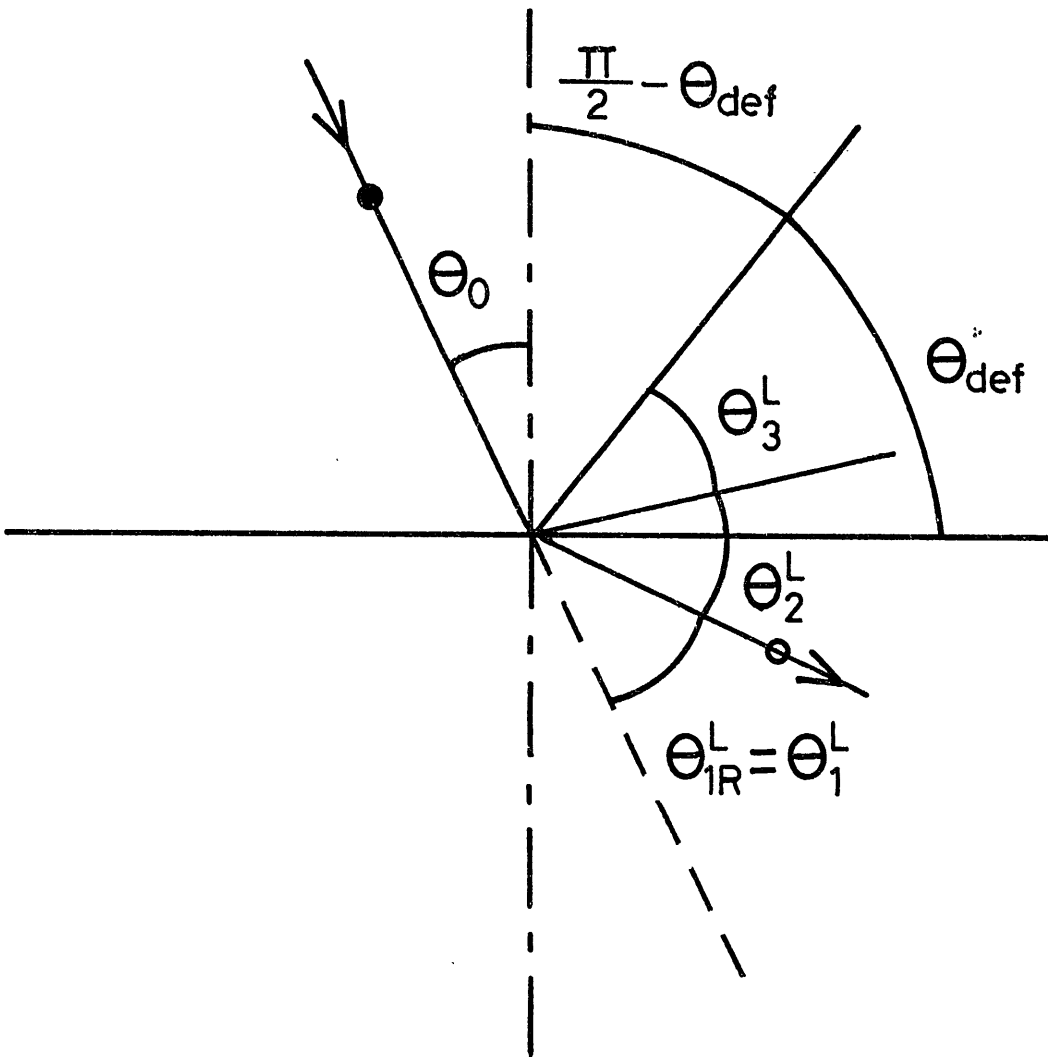


Fig.4 Schematics of the minimum energy loss in a three-collision process (mechanism 1C), where

$$\theta_{1R}^L = \theta_1^L = \theta_2^L = \theta_3^L = \pi/2 - \theta_{\text{def}} = (\pi - \theta_0)/4.$$

MECHANISM 1D.

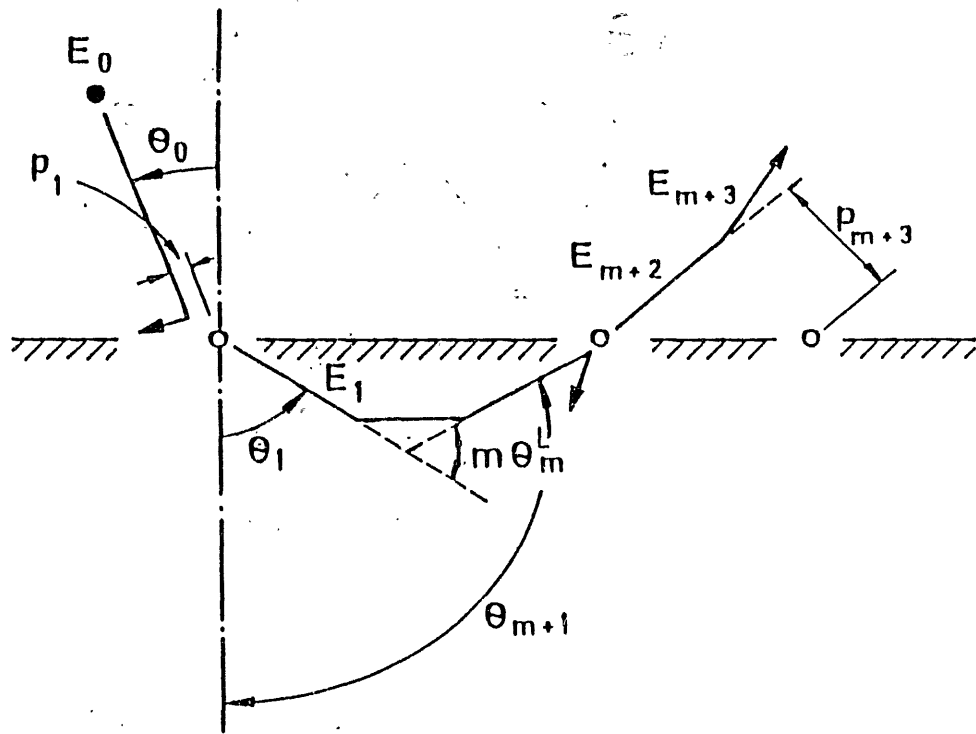


Fig. 5 Schematic representation of the mechanism 1D, where a primary recoil atom is produced at the first collision and the primary recoil atom makes m collisions with target atoms before knocking off a surface atom.

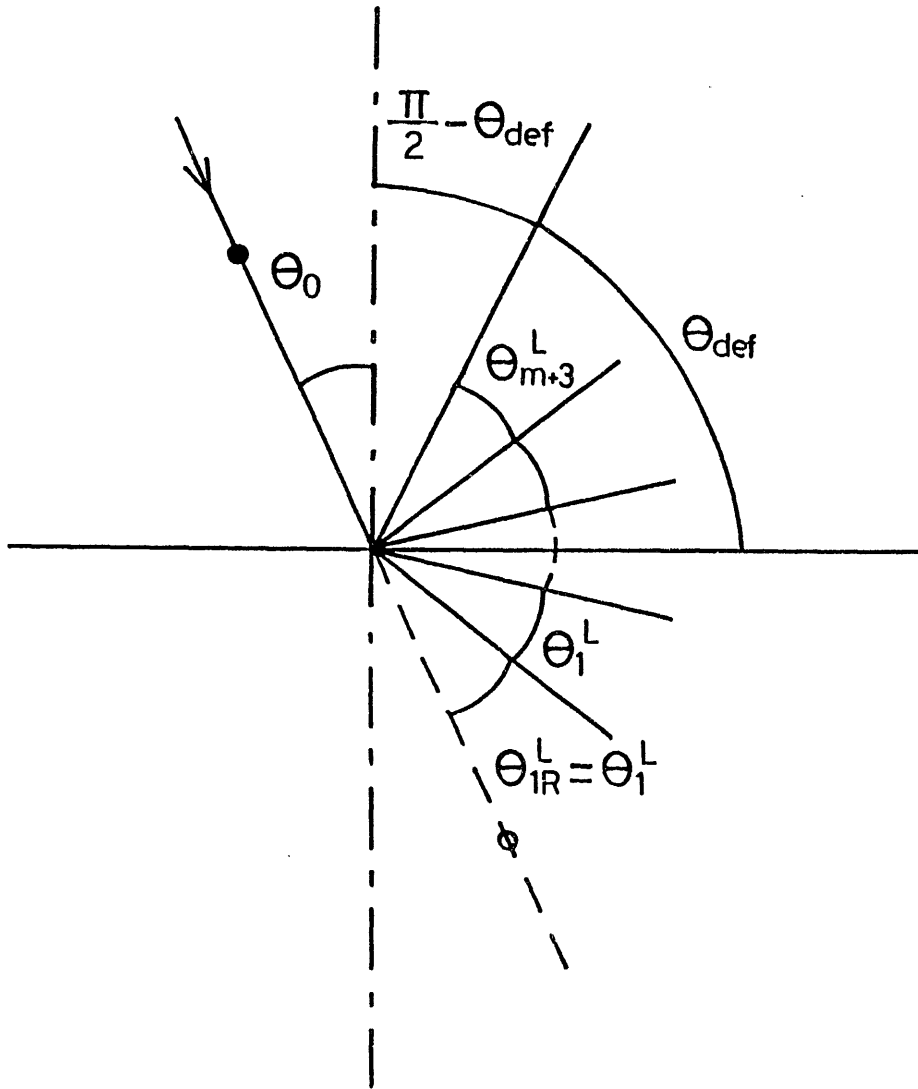


Fig.6 Schematics of the minimum energy loss in a $(m + 1)$ collision process (mechanism 1C), where

$$\theta_{1R}^L = \theta_1^L = \dots = \theta_{m+3}^L = \pi / 2 - \theta_{\text{def}} = (\pi - \theta_0) / (m+4).$$

MECHANISM 2C

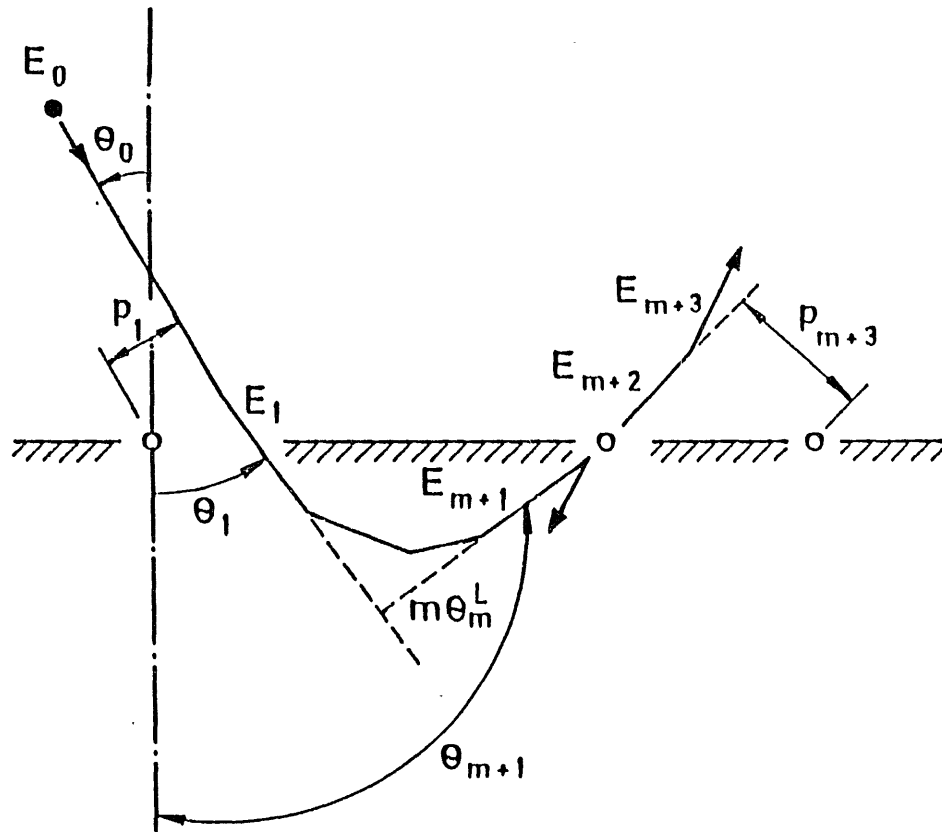


Fig. 7 Schematic representation of the mechanism 2C, where a projectile makes $(m + 1)$ collisions with target atoms before its knocking off a surface atom.

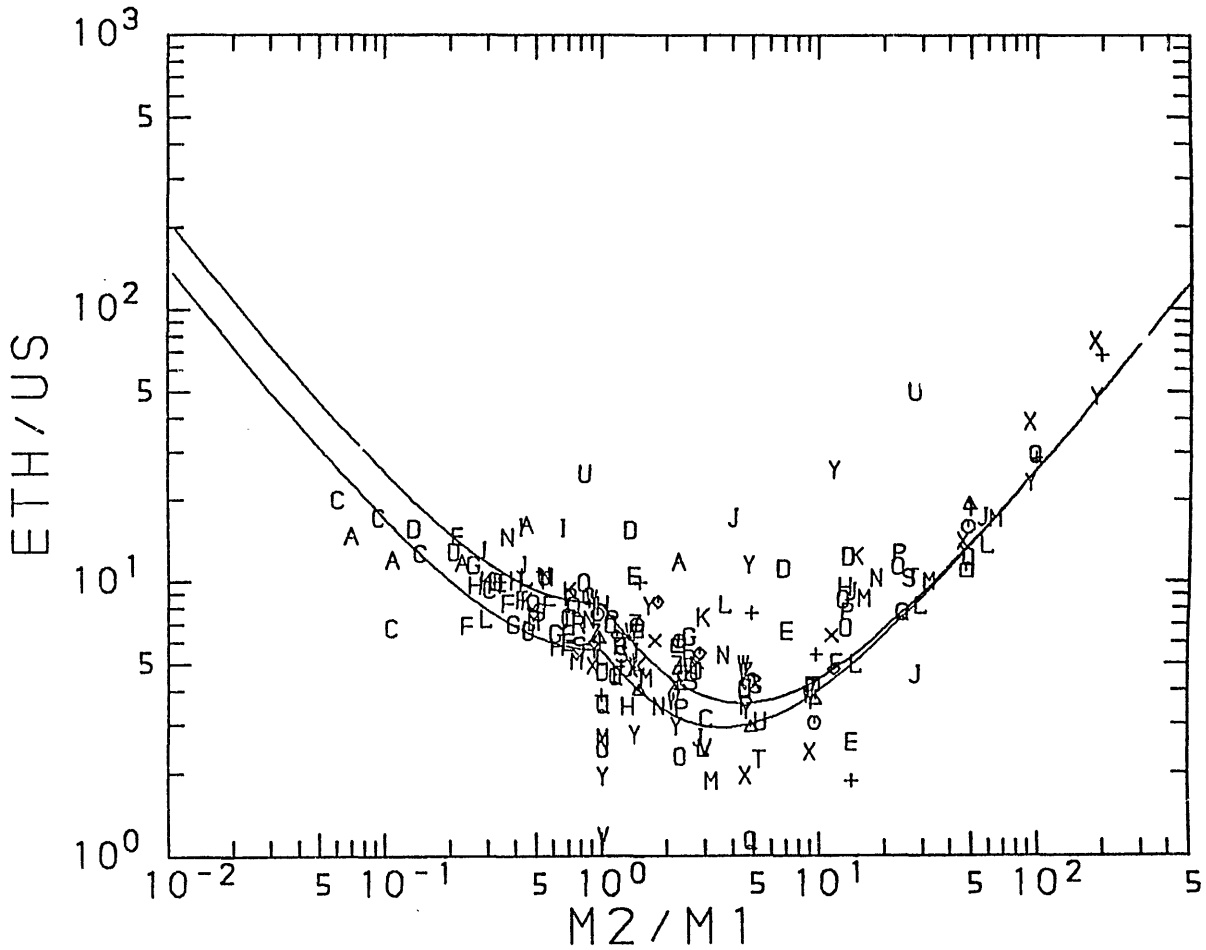


Fig. 8 The mass-ratio dependence of threshold energy at normal incidence for different collision numbers, where the relative threshold energy is plotted. Threshold energy of $m = 1$ in the range of $M_2/M_1 \leq 1$ is calculated from Eq. (52) and that of $m = 2$ from Eq. (58).

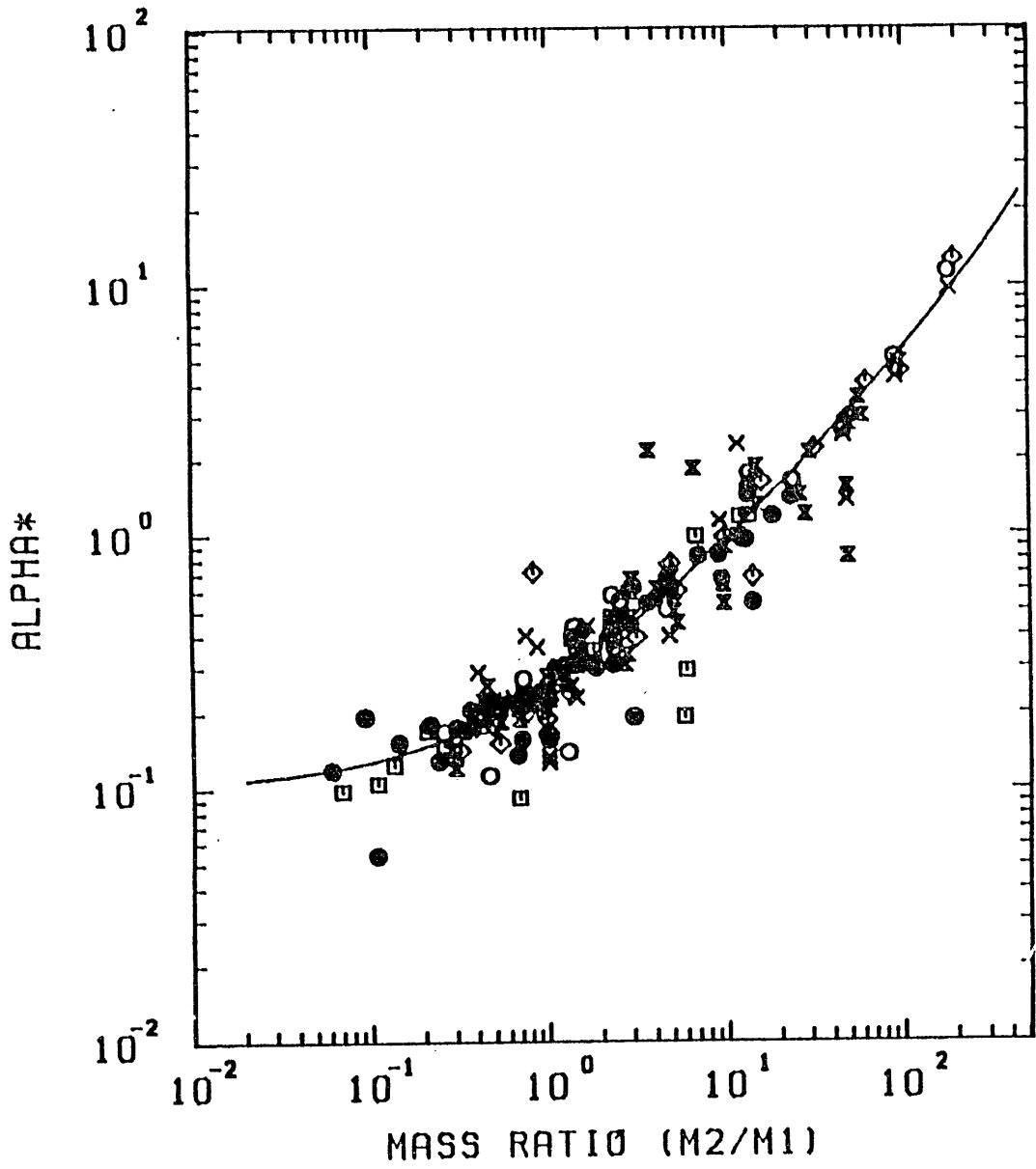


Fig. 9 The mass-ratio dependence of the best fit values of α^* , where the solid one is an empirical relation which is given in Eq. (59).

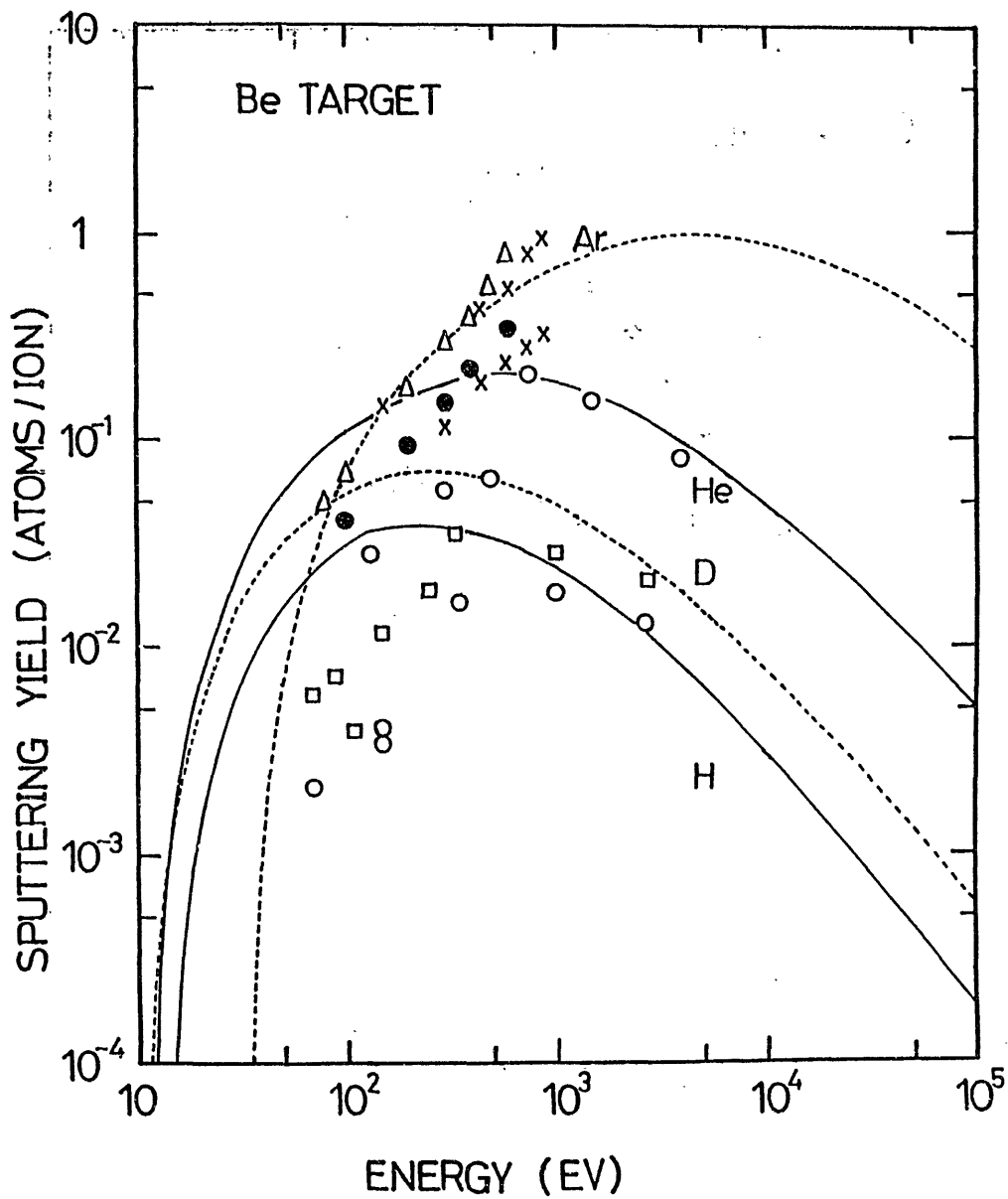


Fig. 10 Comparison between the empirical formula (solid line) and experimental data for Be target in the whole energy region.

H, He(O), D(\square); Roth, Bohdansky, Ottenberger (1979)
 He(\bullet) ; Rosenberg, Wehner (1962)
 He, Ar (x) ; Fetz, Oechsner (1963)
 Ar(Δ) ; Laegreid, Wehner (1961)

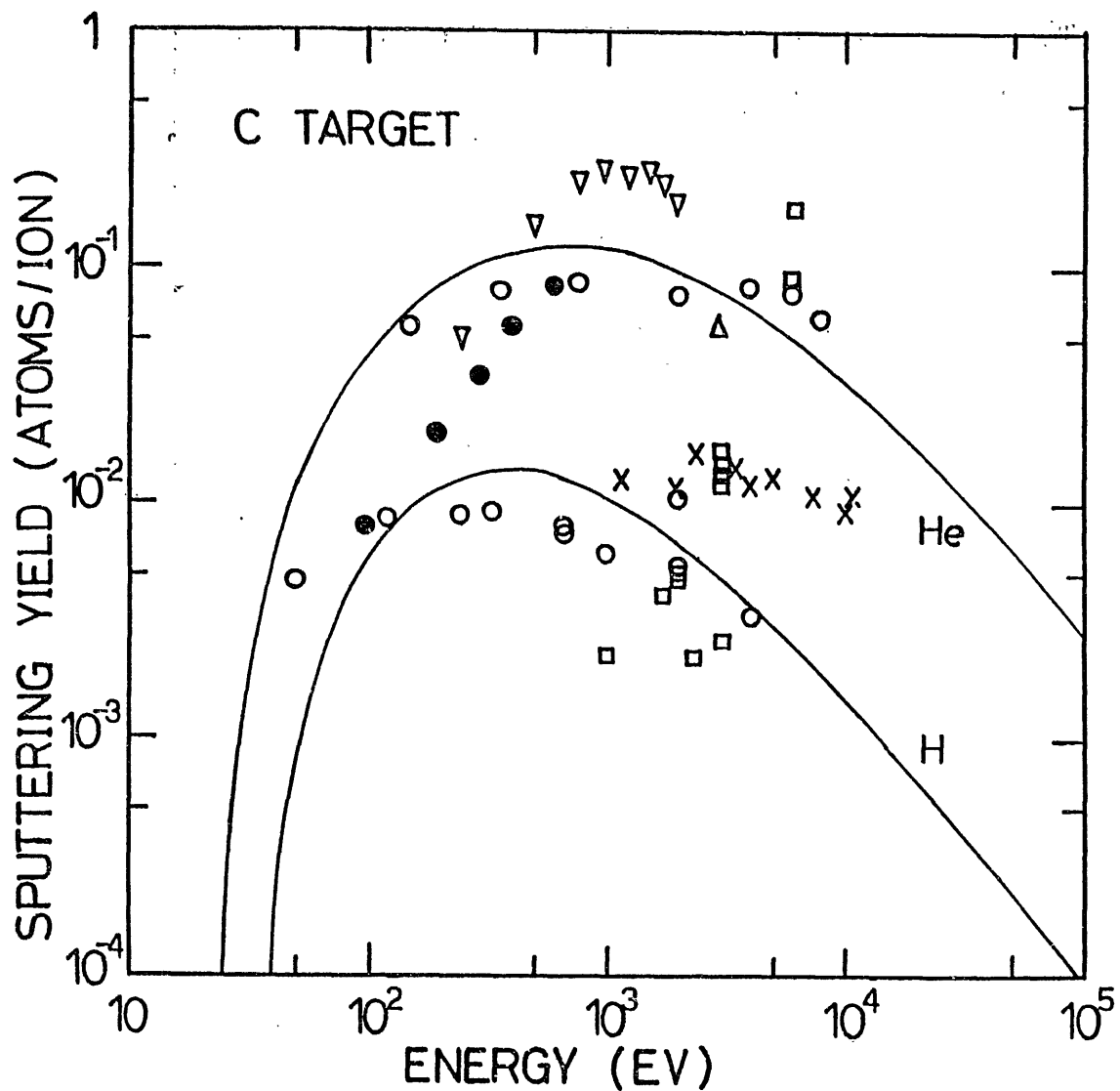


Fig. 11 Comparison between the empirical formula (solid line) and experimental data for H and He ions on C target in the whole energy region.

H, He(□); Behrisch, Bohdanský, Oetjen (1976)
H(x) ; Smith, Meyer, Layton (1976, 1977)
H, He(○); Roth, Bohdanský, Ottenberger (1979)
He(●) ; Rosenberg, Wehner (1962)
He(▽) ; Yamashita, Baba, Kinbara (1980)
He(△) ; Roth, Bohdanský, Wilson (1982)

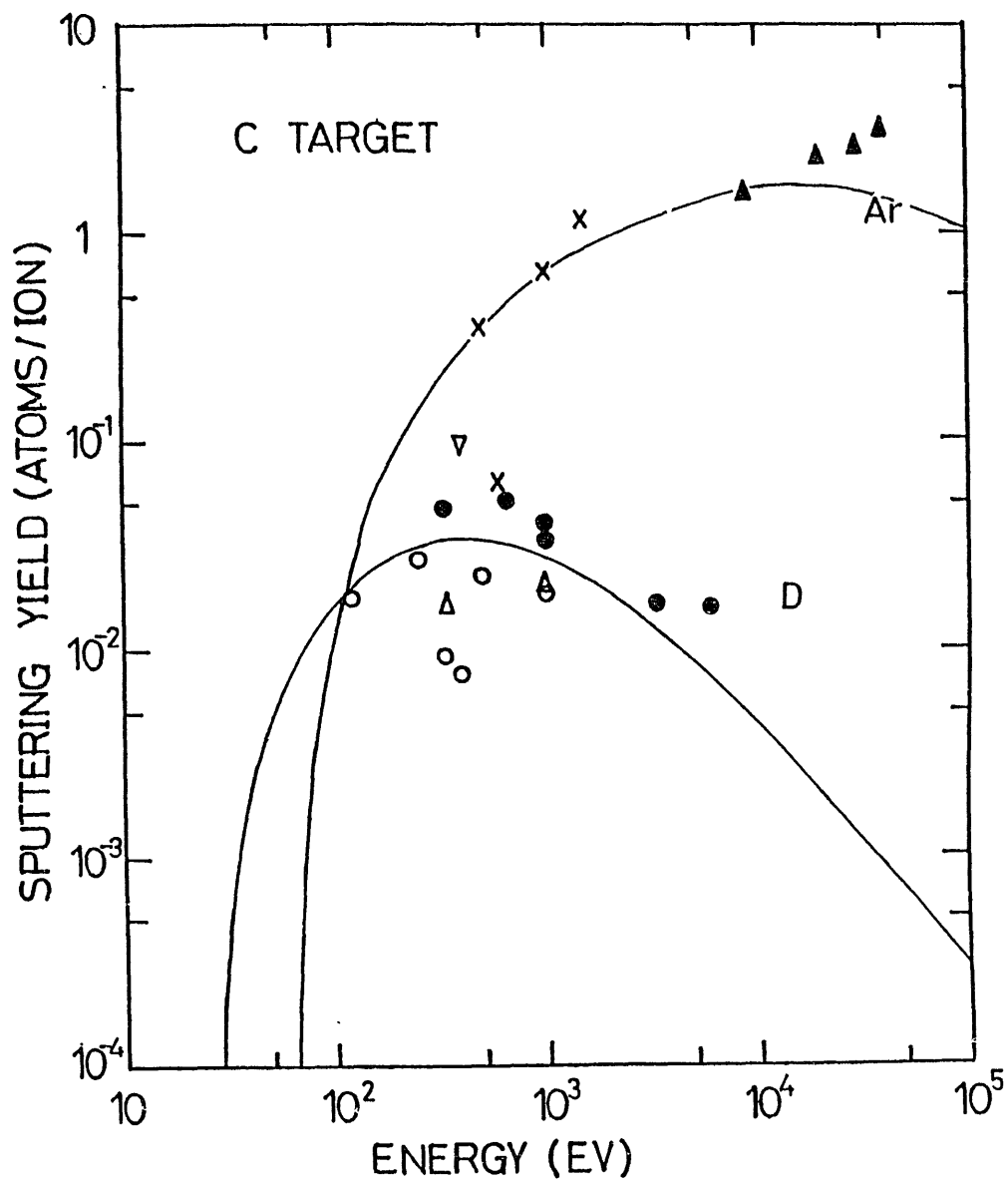


Fig. 12 Comparison between the empirical formula (solid line) and experimental data for D and Ar ions on C target in the whole energy region.

- D(\circ); Roth, Bohdansky, Ottenberger (1979)
- D(\bullet); Baders, Langley, Wilson (1978)
- D(Δ); Roth, Bodansky, Wilson (1982)
- Ar(\times); Smith, Meyer, Layton (1976, 1977)
- Ar(∇); Laegreid, Wehner (1961)
- Ar(\blacktriangle); Betz, Dobrozemaky, Viehbock (1969)

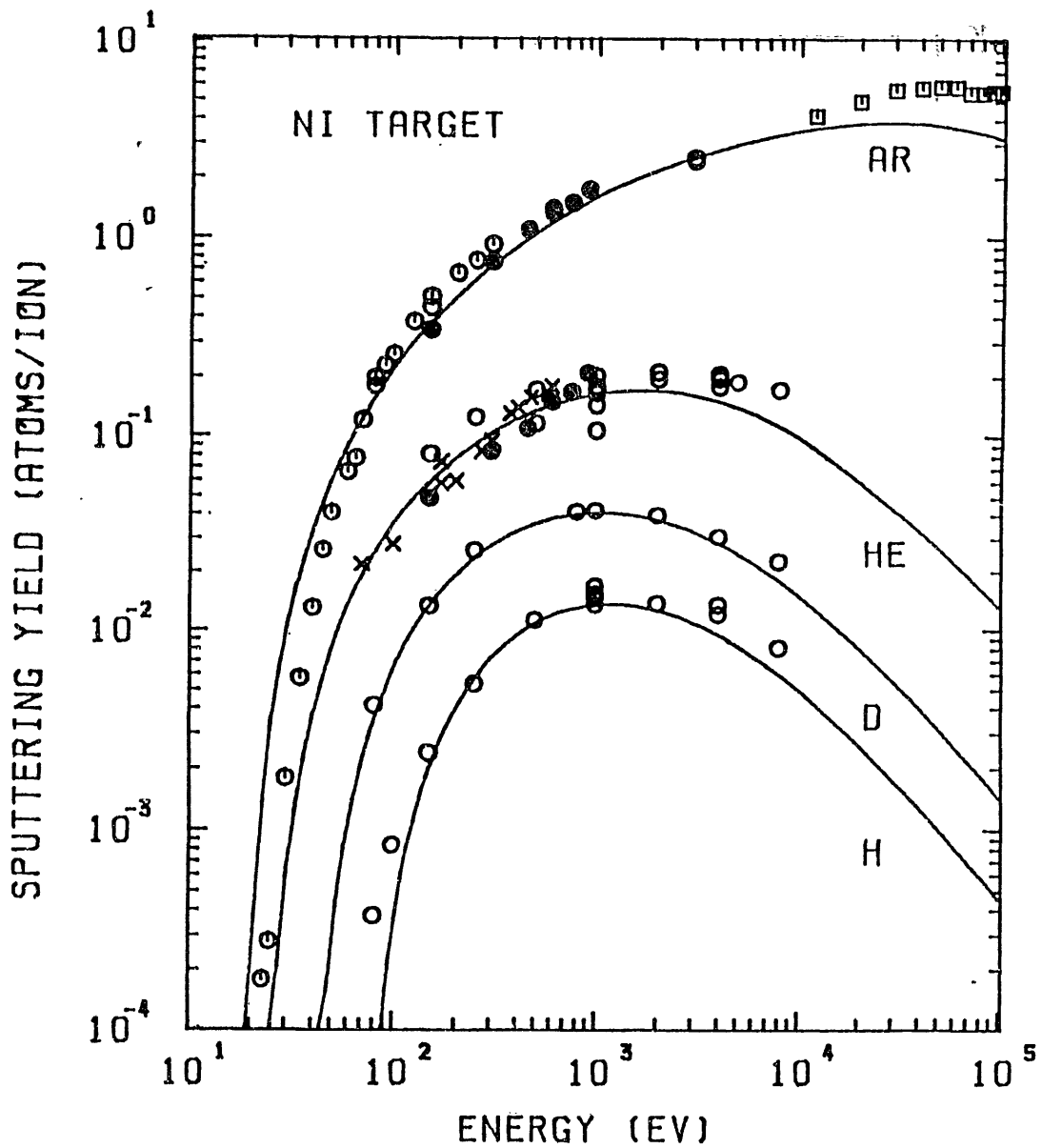


Fig. 13 Comparison between the empirical formula (solid line) and experimental data for Ni target in the whole energy region.

○ : Roth, Bohdanský and Ottenberger (1979)

● : Fetz and Oechsner (1961)

× : Rosenberg and Wehner (1962)

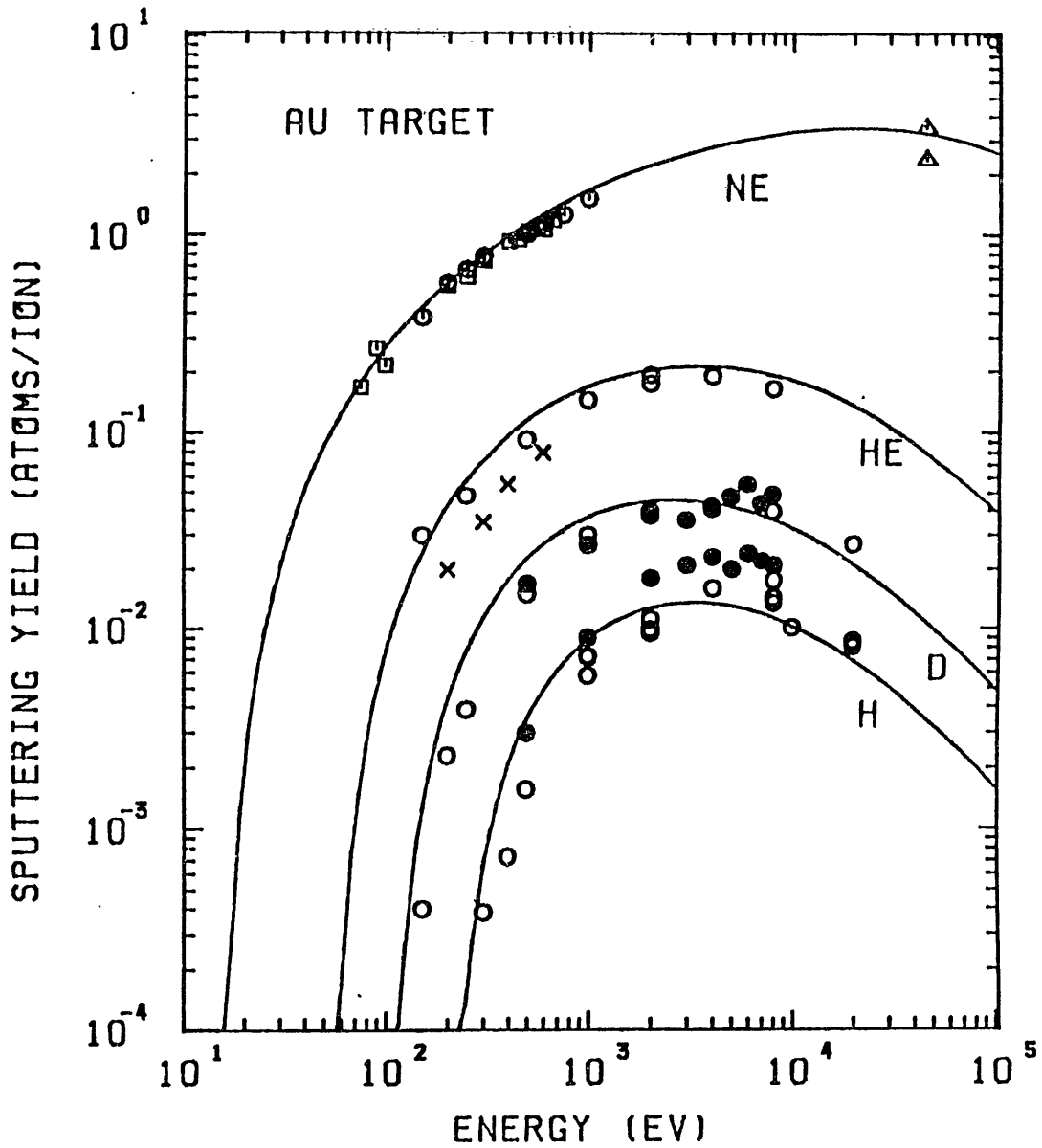


Fig. 14 Comparison between the empirical formula (solid line) and experimental data for Au target in the whole energy region.

- : Roth, Bohdansky and Ottenberger (1979)
- : Furr and Finfgeld (1970)
- × : Rosenberg and Wehner (1962)
- : Laegreid and Wehner (1959)
- : Colligon and Bramham (1970)
- △ : Andersen and Bay (1975)

LIST OF IPPJ-AM REPORTS

- IPPJ-AM-1* "Cross Sections for Charge Transfer of Hydrogen Beams in Gases and Vapors in the Energy Range 10 eV–10 keV"
H. Tawara (1977) [Published in Atomic Data and Nuclear Data Tables 22, 491 (1978)]
- IPPJ-AM-2* "Ionization and Excitation of Ions by Electron Impact –Review of Empirical Formulae–"
T. Kato (1977)
- IPPJ-AM-3 "Grotrian Diagrams of Highly Ionized Iron FeVIII-FeXXVI"
K. Mori, M. Otsuka and T. Kato (1977) [Published in Atomic Data and Nuclear Data Tables 23, 196 (1979)]
- IPPJ-AM-4 "Atomic Processes in Hot Plasmas and X-Ray Emission"
T. Kato (1978)
- IPPJ-AM-5* "Charge Transfer between a Proton and a Heavy Metal Atom"
S. Hiraide, Y. Kigoshi and M. Matsuzawa (1978)
- IPPJ-AM-6* "Free-Free Transition in a Plasma –Review of Cross Sections and Spectra–"
T. Kato and H. Narumi (1978)
- IPPJ-AM-7* "Bibliography on Electron Collisions with Atomic Positive Ions: 1940 Through 1977"
K. Takayanagi and T. Iwai (1978)
- IPPJ-AM-8 "Semi-Empirical Cross Sections and Rate Coefficients for Excitation and Ionization by Electron Collision and Photoionization of Helium"
T. Fujimoto (1978)
- IPPJ-AM-9 "Charge Changing Cross Sections for Heavy-Particle Collisions in the Energy Range from 0.1 eV to 10 MeV I. Incidence of He, Li, Be, B and Their Ions"
Kazuhiko Okuno (1978)
- IPPJ-AM-10 "Charge Changing Cross Sections for Heavy-Particle Collisions in the Energy Range from 0.1 eV to 10 MeV II. Incidence of C, N, O and Their Ions"
Kazuhiko Okuno (1978)
- IPPJ-AM-11 "Charge Changing Cross Sections for Heavy-Particle Collisions in the Energy Range from 0.1 eV to 10 MeV III. Incidence of F, Ne, Na and Their Ions"
Kazuhiko Okuno (1978)
- IPPJ-AM-12* "Electron Impact Excitation of Positive Ions Calculated in the Coulomb-Born Approximation –A Data List and Comparative Survey–"
S. Nakazaki and T. Hashino (1979)
- IPPJ-AM-13 "Atomic Processes in Fusion Plasmas – Proceedings of the Nagoya Seminar on Atomic Processes in Fusion Plasmas Sept. 5-7, 1979"
Ed. by Y. Itikawa and T. Kato (1979)
- IPPJ-AM-14 "Energy Dependence of Sputtering Yields of Monatomic Solids"
N. Matsunami, Y. Yamamura, Y. Itikawa, N. Itoh, Y. Kazumata, S. Miyagawa, K. Morita and R. Shimizu (1980)

- IPPJ-AM-15 “Cross Sections for Charge Transfer Collisions Involving Hydrogen Atoms”
Y. Kaneko, T. Arikawa, Y. Itikawa, T. Iwai, T. Kato, M. Matsuzawa, Y. Nakai,
K. Okubo, H. Ryufuku, H. Tawara and T. Watanabe (1980)
- IPPJ-AM-16 “Two-Centre Coulomb Phaseshifts and Radial Functions”
H. Nakamura and H. Takagi (1980)
- IPPJ-AM-17 “Empirical Formulas for Ionization Cross Section of Atomic Ions for Elec-
tron Collisions –Critical Review with Compilation of Experimental Data–”
Y. Itikawa and T. Kato (1981)
- IPPJ-AM-18 “Data on the Backscattering Coefficients of Light Ions from Solids”
T. Tabata, R. Ito, Y. Itikawa, N. Itoh and K. Morita (1981) [Published in
Atomic Data and Nuclear Data Tables 28, 493 (1983)]
- IPPJ-AM-19 “Recommended Values of Transport Cross Sections for Elastic Collision and
Total Collision Cross Section for Electrons in Atomic and Molecular Gases”
M. Hayashi (1981)
- IPPJ-AM-20 “Electron Capture and Loss Cross Sections for Collisions between Heavy
Ions and Hydrogen Molecules”
Y. Kaneko, Y. Itikawa, T. Iwai, T. Kato, Y. Nakai, K. Okuno and H. Tawara
(1981)
- IPPJ-AM-21 “Surface Data for Fusion Devices – Proceedings of the U.S–Japan Work-
shop on Surface Data Review Dec. 14-18, 1981”
Ed. by N. Itoh and E.W. Thomas (1982)
- IPPJ-AM-22 “Desorption and Related Phenomena Relevant to Fusion Devices”
Ed. by A. Koma (1982)
- IPPJ-AM-23 “Dielectronic Recombination of Hydrogenic Ions”
T. Fujimoto, T. Kato and Y. Nakamura (1982)
- IPPJ-AM-24 “Bibliography on Electron Collisions with Atomic Positive Ions: 1978
Through 1982 (Supplement to IPPJ-AM-7)”
Y. Itikawa (1982) [Published in Atomic Data and Nuclear Data Tables 31,
215 (1984)]
- IPPJ-AM-25 “Bibliography on Ionization and Charge Transfer Processes in Ion-Ion
Collision”
H. Tawara (1983)
- IPPJ-AM-26 “Angular Dependence of Sputtering Yields of Monatomic Solids”
Y. Yamamura, Y. Itikawa and N. Itoh (1983)
- IPPJ-AM-27 “Recommended Data on Excitation of Carbon and Oxygen Ions by Electron
Collisions”
Y. Itikawa, S. Hara, T. Kato, S. Nakazaki, M.S. Pindzola and D.H. Crandall
(1983) [Published in Atomic Data and Nuclear Data Tables 33, 149 (1985)]
- IPPJ-AM-28 “Electron Capture and Loss Cross Sections for Collisions Between Heavy
Ions and Hydrogen Molecules (Up-dated version of IPPJ-AM-20)
H. Tawara, T. Kato and Y. Nakai (1983) [Published in Atomic Data and
Nuclear Data Tables 32, 235 (1985)]

- IPPJ-AM-29 “Bibliography on Atomic Processes in Hot Dense Plasmas”
T. Kato, J. Hama, T. Kagawa, S. Karashima, N. Miyanaga, H. Tawara,
N. Yamaguchi, K. Yamamoto and K. Yonei (1983)
- IPPJ-AM-30 “Cross Sections for Charge Transfers of Highly Ionized Ions in Hydrogen
Atoms (Up-dated version of IPPJ-AM-15)”
H. Tawara, T. Kato and Y. Nakai (1983) [Published in Atomic Data and
Nuclear Data Tables 32, 235 (1985)]
- IPPJ-AM-31 “Atomic Processes in Hot Dense Plasmas”
T. Kagawa, T. Kato, T. Watanabe and S. Karashima (1983)
- IPPJ-AM-32 “Energy Dependence of the Yields of Ion-Induced Sputtering of Monatomic
Solids”
N. Matsunami, Y. Yamamura, Y. Itikawa, N. Itoh, Y. Kazumata, S. Miyagawa,
K. Morita, R. Shimizu and H. Tawara (1983) [Published in Atomic Data and
Nuclear Data Tables 31, 1 (1984)]
- IPPJ-AM-33 “Proceedings on Symposium on Atomic Collision Data for Diagnostics and
Modelling of Fusion Plasmas Aug. 29 – 30, 1983”
Ed. by H. Tawara (1983)
- IPPJ-AM-34 “Dependence of the Backscattering Coefficients of Light Ions upon Angle of
Incidence”
T. Tabata, R. Ito, Y. Itikawa, N. Itoh, K. Morita and H. Tawara (1984)
- IPPJ-AM-35 “Proceedings of Workshop on Synergistic Effects in Surface Phenomena
Related to Plasma-Wall Interactions, May 21 – 23, 1984”
Ed. by N. Itoh, K. Kamada and H. Tawara (1984) [Published in Radiation
Effects 89, 1 (1985)]
- IPPJ-AM-36 “Equilibrium Charge State Distributions of Ions ($Z_1 \geq 4$) after Passage
through Foils – Compilation of Data after 1972”
K. Shima, T. Mikumo and H. Tawara (1985) [Published in Atomic Data and
Nuclear Data Tables 34, 357 (1986)]
- IPPJ-AM-37 “Ionization Cross Sections of Atoms and Ions by Electron Impact”
H. Tawara, T. Kato and M. Ohnishi (1985)
- IPPJ-AM-38 “Rate Coefficients for the Electron-Impact Excitations of C-like Ions”
Y. Itikawa (1985)
- IPPJ-AM-39 “Proceedings of the Japan-U.S. Workshop on Impurity and Particle Control,
Theory and Modeling, Mar. 12 – 16, 1984”
Ed. by T. Kawamura (1985)
- IPPJ-AM-40 “Low-Energy Sputterings with the Monte Carlo Program ACAT”
Y. Yamamura and Y. Mizuno (1985)
- IPPJ-AM-41 “Data on the Backscattering Coefficients of Light Ions from Solids (a
Revision)”
R. Ito, T. Tabata, N. Itoh, K. Morita, T. Kato and H. Tawara (1985)

- IPPJ-AM-42 “Stopping Power Theories for Charged Particles in Inertial Confinement Fusion Plasmas (Emphasis on Hot and Dense Matters)”
S. Karashima, T. Watanabe, T. Kato and H. Tawara (1985)
- IPPJ-AM-43 “The Collected Papers of Nice Project/IPP, Nagoya”
Ed. by H. Tawara (1985)
- IPPJ-AM-44 “Tokamak Plasma Modelling and Atomic Processes”
Ed. by T. Kawamura (1986)
- IPPJ-AM-45 Bibliography of Electron Transfer in Ion-Atom Collisions
H. Tawara, N. Shimakura, N. Toshima and T. Watanabe (1986)
- IPPJ-AM-46 “Atomic Data Involving Hydrogens Relevant to Edge Plasmas”
H. Tawara, Y. Itikawa, Y. Itoh, T. Kato, H. Nishimura, S. Ohtani, H. Takagi, K. Takayanagi and M. Yoshino (1986)
- IPPJ-AM-47 “Resonance Effects in Electron-Ion Collisions”
Ed. by H. Tawara and G. H. Dunn (1986)
- IPPJ-AM-48 “Dynamic Processes of Highly Charged Ions (Proceedings)”
Ed. by Y. Kanai and S. Ohtani (1986)
- IPPJ-AM-49 “Wavelengths of K X-Rays of Iron Ions”
T. Kato, S. Morita and H. Tawara (1987)
- IPPJ-AM-50 “Proceedings of the Japan-U.S. Workshop P-92 on Plasma Material Interaction/High Heat Flux Data Needs for the Next Step Ignition and Steady State Devices, Jan. 26 – 30, 1987”
Ed. by A. Miyahara and K. L. Wilson (1987)
- IPPJ-AM-51 “High Heat Flux Experiments on C-C Composite Materials by Hydrogen Beam at the 10MW Neutral Beam Injection Test Stand of the IPP Nagoya”
H. Bolt, A. Miyahara, T. Kuroda, O. Kaneko, Y. Kubota, Y. Oka and K. Sakurai (1987)
- IPPJ-AM-52 “Energy Dependence of Ion-Induced Sputtering Yields of Monatomic Solids in the Low Energy Region”
N. Matsunami, Y. Yamamura, N. Itoh, H. Tawara and T. Kawamura (1987)

Available upon request to Research Information Center, Institute of Plasma Physics, Nagoya University, Nagoya 464, Japan, except for the reports noted with*.